Contribution of Cutinase Serine 42 Side Chain to the Stabilization of the Oxyanion Transition State[†,‡]

Anne Nicolas,[§] Maarten Egmond,[∥] C. Theo Verrips,[∥] Jakob de Vlieg,[∥] Sonia Longhi,[§] Christian Cambillau,*[,§] and Chrislaine Martinez[§]

Laboratoire de Cristallographie et Cristallisation des Macromolécules Biologiques, URA1296-CNRS, IFR1, 31 Chemin J. Aiguier, 13402 Marseille cedex 09, France, and Unilever Research Laboratorium, Olivier van Noortlann 120, 3133 AT, Vlaardingen, The Netherlands

Received July 10, 1995; Revised Manuscript Received November 1, 1995[⊗]

ABSTRACT: Cutinase from the fungus *Fusarium solani pisi* is a lipolytic enzyme able to hydrolyze both aggregated and soluble substrates. It therefore provides a powerful tool for probing the mechanisms underlying lipid hydrolysis. Lipolytic enzymes have a catalytic machinery similar to those present in serine proteinases. It is characterized by the triad Ser, His, and Asp (Glu) residues, by an oxyanion binding site that stabilizes the transition state via hydrogen bonds with two main chain amide groups, and possibly by other determinants. It has been suggested on the basis of a covalently bond inhibitor that the cutinase oxyanion hole may consist not only of two main chain amide groups but also of the Ser42 Oγ side chain. Among the esterases and the serine and the cysteine proteases, only *Streptomyces scabies* esterase, subtilisin, and papain, respectively, have a side chain residue which is involved in the oxyanion hole formation. The position of the cutinase Ser42 side chain is structurally conserved in *Rhizomucor miehei* lipase with Ser82 Oγ, in *Rhizopus delemar* lipase with Thr83 Oγ1, and in *Candida antartica* B lipase with Thr40 Oγ1. To evaluate the increase in the tetrahedral intermediate stability provided by Ser42 Oγ, we mutated Ser42 into Ala. Furthermore, since the proper orientation of Ser42 Oγ is directed by Asn84, we mutated Asn84 into Ala, Leu, Asp, and Trp, respectively, to investigate the contribution of this indirect interaction to the stabilization of the oxyanion hole. The S42A mutation resulted in a drastic decrease in the activity (450-fold) without significantly perturbing the three-dimensional structure. The N84A and N84L mutations had milder kinetic effects and did not disrupt the structure of the active site, whereas the N84W and N84D mutations abolished the enzymatic activity due to drastic steric and electrostatic effects, respectively.

Cutinase from the fungus *Fusarium solani pisi* is a lipolytic enzyme which acts on both monomeric and aggregated triglycerides but which shows no enhancement of its activity in the presence of a lipid−water interface (Kolattukudy, 1984; Lauwereys et al., 1991). This enzyme has been well studied: its X-ray structure has been refined at 1.25 Å resolution (Martinez, 1992) and is being extended up to 1.0 Å resolution (S. Longhi et al., unpublished results). Around 40 X-ray structures of cutinase mutants and inhibitor conjugates have been solved to date (S. Longhi et al. and Nicolas et al., unpublished results). Cutinase is also an excellent model for kinetically probing the lipolytic machinery due to its ability to hydrolyze soluble substrates.

In recent years, the amount of knowledge available about lipase structure and enzymatic structure−function has increased tremendously (Brady et al., 1990; Winkler et al., 1990; Brzozowski et al., 1991; Schrag et al., 1991; van Tilbeurgh et al., 1992, 1993; Grochulski et al., 1993; Bourne et al., 1994; Noble et al., 1994; Derewenda et al., 1994; Uppenberg et al., 1994; Jaeger et al., 1994; Egloff et al., 1995). These soluble enzymes have in common their structure, the α/β hydrolase fold (Ollis et al., 1992) and the surface loop, called the "lid", covering their active site. During the catalytic process, a structural rearrangement of this lid occurs, allowing the substrate to dock in the active site. In most cases, optimal oxyanion hole geometry is achieved only via this structural change. These phenomena have been thought to provide the structural explanation for the activation of lipases which occurs in the presence of a lipid−water interface. Among these lipolytic enzymes, cutinase has unique properties since its active site serine is not covered by a lid and its oxyanion hole is preformed (Martinez et al., 1994). These two facts explain why it does not display any interfacial activation in the presence of aggregated substrate (Martinez et al., 1992).

Using phosphorylating agents makes it possible to block the esterases, lipases, and various serine-dependant hydrolases reaction mechanism at the acylation step via the formation of a tetrahedral intermediate (Kraut, 1977). The negatively charged oxygen of the tetrahedral intermediate, originating from the substrate oxyanion, is stabilized by hydrogen bonds with two peptide NH groups of the main chain enzyme, leading to the formation of the so-called oxyanion hole. The oxyanion hole is a common feature which is present in all the known serine proteases (Kraut, 1977; Warshel et al., 1989), esterases (Sussman et al., 1991;

[†] This study was supported by the EC BRIDGE-T "Lipase" project (BIOT CT91-023), the CNRS-IMABIO program, and the PACA region.

[‡] Coordinates have been deposited with the Brookhaven Protein Data Bank under file names 1FFA, 1FFB, 1FFC, 1FFD, and 1FFE.

* Corresponding author. Phone: (33) 91 16 45 01. Fax: (33) 91 16 45 36. E-mail: cambilau@ibsm.cnrs-mrs.fr.

[§] CNRS.

[∥] Unilever Research Laboratorium.

[⊗] Abstract published in *Advance ACS Abstracts,* December 15, 1995.

Wei et al., 1995), lipases (Brady et al., 1990; Brzozowski et al., 1991; van Tilbeurg et al., 1993; Grochulski et al., 1993; Derewenda et al., 1994; Egloff et al., 1995), and serine carboxypeptidases (Liao & Remington, 1990). These hydrogen bonds seem to accelerate the reaction by distorting the ground state acyl-enzyme structure along the enzymatic pathway (Pauling, 1946). A tetrahedrically distorted carbonyl exists in complexed enzymes, and this distortion is essential for strong oxyanion hole hydrogen bonds to be formed. The strength of the hydrogen bonds in the acyl-enzyme between the carbonyl and the oxyanion hole has been found to positively be correlated with an increase in the rate of deacylation (Whiting & Peticolas, 1994).

The three-dimensional structure of cutinase inhibited with diethyl paranitrophenyl phosphate (E600)[1] was recently solved (Martinez et al., 1994). The inhibitor, which blocks the reaction at the acylation step, mimicks the first tetrahedral intermediate, thus making it possible to identify the cutinase oxyanion hole components. The fact that cutinase, like serine proteases, shows very little change in the position of its catalytic residues as the result of the complex formation suggests that, in its native state, the active site may be complementary to tetrahedral reaction intermediates. The oxyanion hole of cutinase can be described in terms of the interactions between the phosphate inhibitor, E600, and several main chain and side chain cutinase atoms: Ser42 N, Gln121 N, and Ser42 Oγ interact directly with the oxyanion. Asn84 Nδ2 and Gln121 Nϵ2 maintain Ser42 Oγ in the proper orientation for the hydrogen bonding of the oxyanion to occur. Ser42 therefore occupies a central position in the oxyanion hole pocket, not only because its main chain NH group is a hydrogen donor contributing to the oxyanion formed but also because its side chain Oγ atom is within hydrogen bonding distance from the oxyanion. We therefore mutated this residue into an alanine which is unable to hydrogen bond to the oxyanion. Point mutants that selectively disrupt each of these interactions were designed in order to assess the potential function of the Ser42 side chain as part of the cutinase oxyanion hole. Mutating Ser42 into Ala would cancel the direct interaction between the oxyanion and residue 42 side chain Oγ. One of the two residues belonging to the second shell were also mutated: Asn84 into Ala, Leu, Trp, and Asp. Structural modifications of these cutinase mutants were evaluated as regards their ability to hydrolyze paranitrophenyl-butyrate (pnp-butyrate) in solution, since cutinase is able to hydrolyze this soluble substrate. Any secondary effects originating from interfacial activation can therefore be dissociated from the primary effects on the integrity of the oxyanion hole.

MATERIALS AND METHODS

Cutinase Site-Directed Mutagenesis. A 670 base pair synthetic gene of normal *F. solani pisi* cutinase obtained by cassette assembly was cloned into the *Eco*RI and *Hin*dIII restriction sites of a pUC19 derived vector (Unilever vector) prior to the subcloning steps. The gene was expressed in *Saccharomyces cerevisiae* by cloning the modified gene into the *Sac*I and *Hin*dIII sites of a MIRY plasmid (Orr-Weaver & Szostak, 1983; Lopes et al., 1989) containing the Pgal7 promotor. Site-directed mutagenesis was performed using the overlap extension polymerase chain reaction method (PCR; Dulau et al., 1989; Ho et al., 1989). The following experimental conditions were used: approximately 10 ng of pUC19 plasmid DNA harboring the cutinase gene was used as a template for PCR in a total volume of 50 μL containing 1 unit of Taq polymerase (Pharmacia) (Kadowaki et al., 1989), 50 mM NaCl, 10 mM Tris-HCl, pH 8.3, 2 mM $MgCl_2$, 200 μM dNTPs (Pharmacia), and 100 pmol of each primer and covered with 100 μL of light mineral oil. PCR was performed in 30 cycles, each of which consisted of a denaturing step at 95 °C, a primer annealing step at 58 °C for 1.5 min, and an extension step at 72 °C for 1.5 min using a Perkin Elmer cetus DNA thermal cycler. The amplified DNA fragments were then subcloned into the shuttle vector, thus replacing the native sequence.

All the constructs were characterized by performing sequence analysis on the complete cutinase insert. Synthetic fluorescent oligonucleotides were synthesized (Smith et al., 1985) in order to perform fluorescent automatic sequencing (Smith et al., 1986) combined with Sanger's dideoxynucleotide termination method (Sanger et al., 1980).

Purification of the Mutants. A volume of 25−125 mL of SP Sepharose fast flow gel (17-0729-01, Pharmacia) was added to each variant solution (0.01 M sodium acetate, 0.025 M NaCl, pH 4.6). The cutinase mutants were eluted from the strong cation exchange column with 0.01 M TEA/HCl and 0.025 M NaCl, pH 9, at a flow rate of 7 mL/min. The eluate was filtered through a DEAE-cellulose (DE 52, Whatman) and adjusted to pH 9 before being loaded onto a Q Sepharose fast flow (17-0510-01, Pharmacia) column. The elution was carried out at pH 9 with a linear NaCl gradient of 0.025−0.4 M and a flow rate of 7 mL/min. The last purification step consisted of an affinity chromatography using a Con-A Sepharose 4B (17-0440-01, Pharmacia) column in order to remove any glycosylated fractions. Electrospray mass spectrometry was used to confirm the identity of the variants obtained and to check whether any residual glycosylation was present. After dialysis and lyophilization, each mutant was dissolved at 1 mg/mL in 20 mM Tris-HCl and 10 mM NaCl, pH 9, to measure the specific activity on triolein stabilized with gum arabic (Sigma).

Activity Measurements. The enzymic activities of the mutants were quantified in duplicate using pnp-Butyrate in butanol 100% as the substrate, at concentrations ranging from 0.1 to 1 mM. Assays were performed in 20 mM Tris-HCl, pH 9, at 30 °C, containing 1 or 0.1 mg/mL of each variant. The reaction rates were determined by measuring the rate of paranitrophenol release at 405 nm ($\epsilon = 15\,300\ M^{-1}\ cm^{-1}$). The kinetic constants, V_M and k_{cat}, determined from nonlinear regresssion curves (Duggleby, 1981) based on the initial rate data, are summarized in Table 1.

Crystallization and Structure Determination of the Mutants. The cutinase mutants were crystallized using the vapour diffusion technique (Matthews, 1968), under conditions similar to those used with the wild-type enzyme (Abergel et al., 1990). Crystals were obtained in 100 mM Hepes, pH 7, using PEG 6000 as precipitant in the range of 10−20%, except for N84L, which required lower PEG

[1] Abbreviations: E600, diethyl paranitrophenyl phosphate; pnp, paranitrophenyl; RmL, *Rhizomucor miehei* lipase; HPL, human pancreatic lipase; RdL, *Rhizopus delemar* lipase; PcL, *Penicillium camembertii* lipase; HlL, *Humicola lanuginosa* lipase; CaBL, *Candida antartica* B lipase; CBZ-Phe-Arg-MCA, carbobenzoxy-L-phenyl-alanyl-(7-amino-4-methylcoumarinyl)-L-arginine.

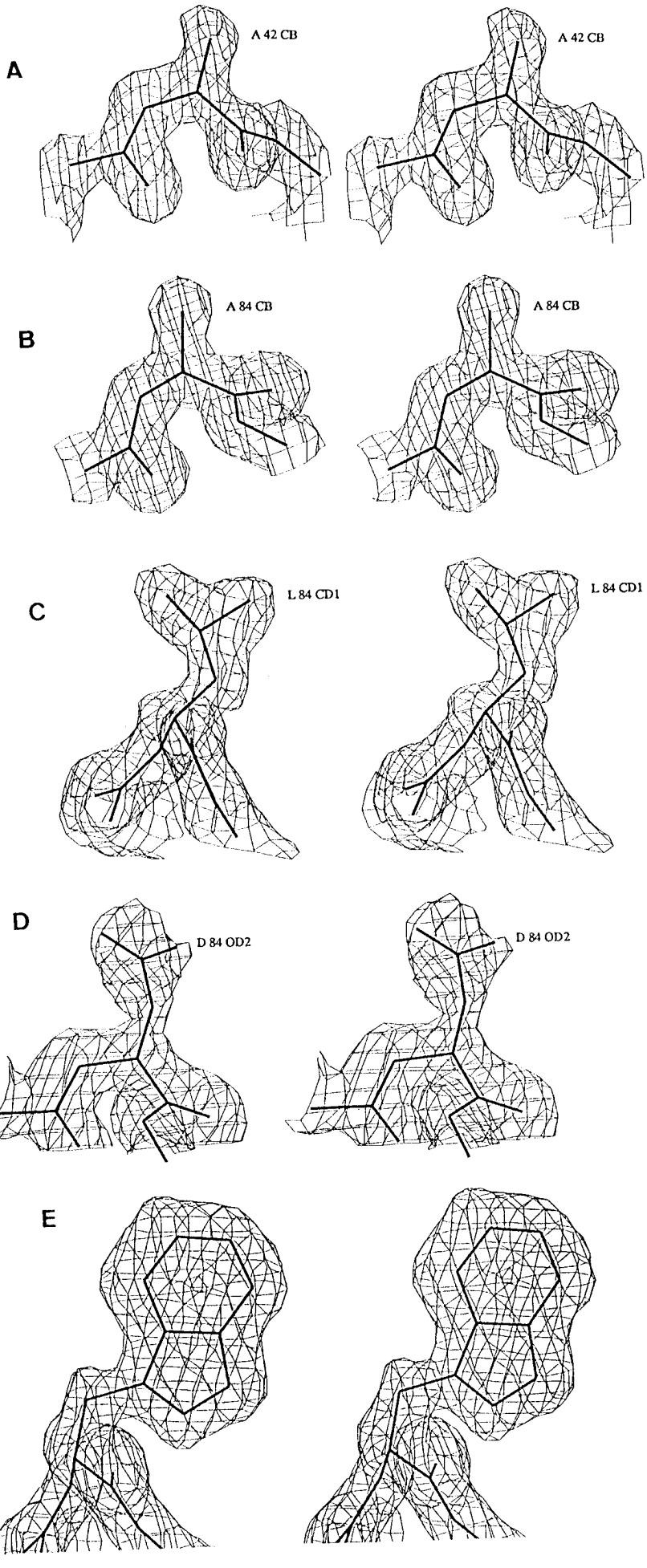
A
A 42 CB
A 42 CB
B
A 84 CB
A 84 CB
C
L 84 CD1
L 84 CD1
D
D 84 OD2
D 84 OD2
E

Table 1: Steady-State Kinetic Parameters of Native and Mutants Cutinase during the Hydrolysis of pnp-Butyrate

	k_{cat} (s^{-1})	k_{cat}/K_M (s^{-1} mM^{-1})	% residual activity
WT	1800	2647	100.00
S42A	4	12	0.22
N84A	478	1062	26.5
N84L	55	190	3.00
N84W	2	6	0.11
N84D	2.5	19	0.16

concentrations (2−5%). S42A and N84A-L-W crystals were found to be isomorphous to the wild-type enzyme and to have space group $P2_1$ and the following cell parameters: 35.12 Å, 67.36 Å, 37.05 Å, and $\beta = 94°$. N84D still crystallized in $P2_1$ but had different cell parameters: 36.95 Å, 64.23 Å, 37.11 Å, and $\beta = 116.12°$.

X-ray diffraction data were measured on a 18 cm MAR-Research Imaging plate detector (Mar-research, Hamburg, Germany) mounted on a Rigaku RU200 rotating anode (running at 40 kV × 80 mA). The data were reduced with the Imaging plate version of the XDS program (Kabsch, 1988) and the CCP4 program package (SERC Daresbury Laboratory, UK). Data reductions are given in Table 2.

The structure of N84D mutant was solved by performing molecular replacement using the AMoRe program (Navaza, 1994). The coordinates of the native cutinase were placed in a $P1$ cell having the dimensions $a = b = c = 60$ Å. The rotation function was calculated in the resolution range of 20−4 Å with a Patterson integration radius of 30 Å. Solution 2 gave the Euler angles $\theta_1 = 175.68°$, $\theta_2 = 91.56°$, and $\theta_3 = 291.59°$ and the translation vectors $X_1 = 21.33$ Å, $X_2 = 22.50$ Å, and $X_3 = 59.85$ Å with a correlation cœfficient of 80.4% and a R factor of 28.1%.

We used the 3.1 version of the X-PLOR program package (Brünger, 1992) for the crystallographic refinement and the structural analysis, which involved the Engh−Huber force field (Engh & Huber, 1991). The starting model was taken from the cutinase structure refined at 1.25 Å resolution (Martinez, 1992a). A standard simulated annealing protocol (Brünger, 1989) was first used to refine the variant structures. Forty cycles of conjugate gradient minimization were followed by molecular dynamics (0.001 ps at 300 K), 360 steps of conjugate gradient minimization, and 40 cycles of restrained individual B factor refinement. Reflections between 6.0 Å and the highest resolution (Table 2) were used in the refinement, and ($2F_oF_c$) and (F_oF_c) difference maps were calculated between 20.0 and 1.6 Å resolution. These were inspected on Silicon Graphics workstations using the TURBO graphics program (Roussel & Cambillau, 1991). ($2F_oF_c$) electron density maps corresponding to the mutated residues are given in Figure 1. Luzzati plots gave an average estimated error of 0.07 Å.

Structural alignment was performed with the RIGID option of the TURBO graphics program (Roussel & Cambillau, 1991). All mutant Cα atoms located at less than 0.5 Å from their native corresponding ones were included in the least-squares adjustment procedure. The rmsd values resulting from this procedure, calculated on the basis of 194 Cα, were 0.043 Å (S42A), 0.068 Å (N84A), 0.037 Å (N84L), 0.077 Å (N84W), and 0.187 Å with N84D, which is the only one belonging to a different crystal form.

RESULTS

Three levels of interaction between the enzyme and the phosphate inhibitor can be distinguished in the area of the cutinase oxyanion hole (Figure 2A): in the first shell, Ser42 N, Gln121 N, and Ser42 Oγ interact directly with the oxyanion (P)-O3 oxygen. The interactions of (P)-O3 with Ser42 N (2.86 Å) and Gln121 N (2.87 Å) in the oxyanion hole are tight and equidistant. A third hydrogen bond, established with the Ser42 Oγ side chain, is shorter (2.68 Å). The second interaction shell comprises Asn84 Nδ2 and Gln121 Nϵ2 atoms, which are hydrogen bond donors and as such maintain the Ser42 hydroxyl group in the appropriate orientation for the hydrogen bonding of the oxyanion atom to take place. In the third shell, tetracoordinated water molecules properly orientate Asn84 Oδ1 and Gln121 Oϵ1 side chain atoms. The wild-type cutinase catalytic pocket contains a water molecule located close to the active serine,

Table 2: Data Collection and Final Refinement Statistics of Cutinase Mutants

	S42A	N84A	N84L	N84W	N84D
		Data Collection			
	XDS	XDS	XDS	MOSFLM	XDS
resolution limit (Å)	1.69	1.69	1.75	1.69	1.75
data completion ($I/\sigma[I] > I$)	89.9	95.3	89.3	92.9	93.3
% for which $I > 3\sigma[I]$	84.5	91.7	82.1	94.7	85.1
number of unique reflections	17 069	18 092	15 547	17 226	15 053
number of collected reflections	56 062	60 359	55 204	50 283	50 443
R_{sym} (all reflections)	3.9	2.9	4.2	5.7	4.5
		Refinement			
total number of reflections	16 806	17 888	15 276	16 762	14 687
total number of atoms	1776	1773	1776	1783	1776
total number of water molecules	352	309	325	283	230
final R factor	13.5	13.7	14.0	14.4	14.7
B factors (Å^2)					
main chains	9.7	9.9	9.7	12.8	9.2
side chains	24.9	23.2	21.6	24.7	18.9
solvent	44.9	38.4	39.4	40.4	37.1
rms deviations from ideal values					
bonds (Å)	0.008	0.009	0.009	0.01	0.008
angles (deg)	1.403	1.426	1.4	1.465	1.458

FIGURE 1: Stereoview of ($2F_o - F_c$) electron density maps around the mutated residues: S42A (A), N84A (B), N84L (C), N84D (D), and N84W (E). The electron density is contoured at the level of 1.0σ (graphics program TURBO).

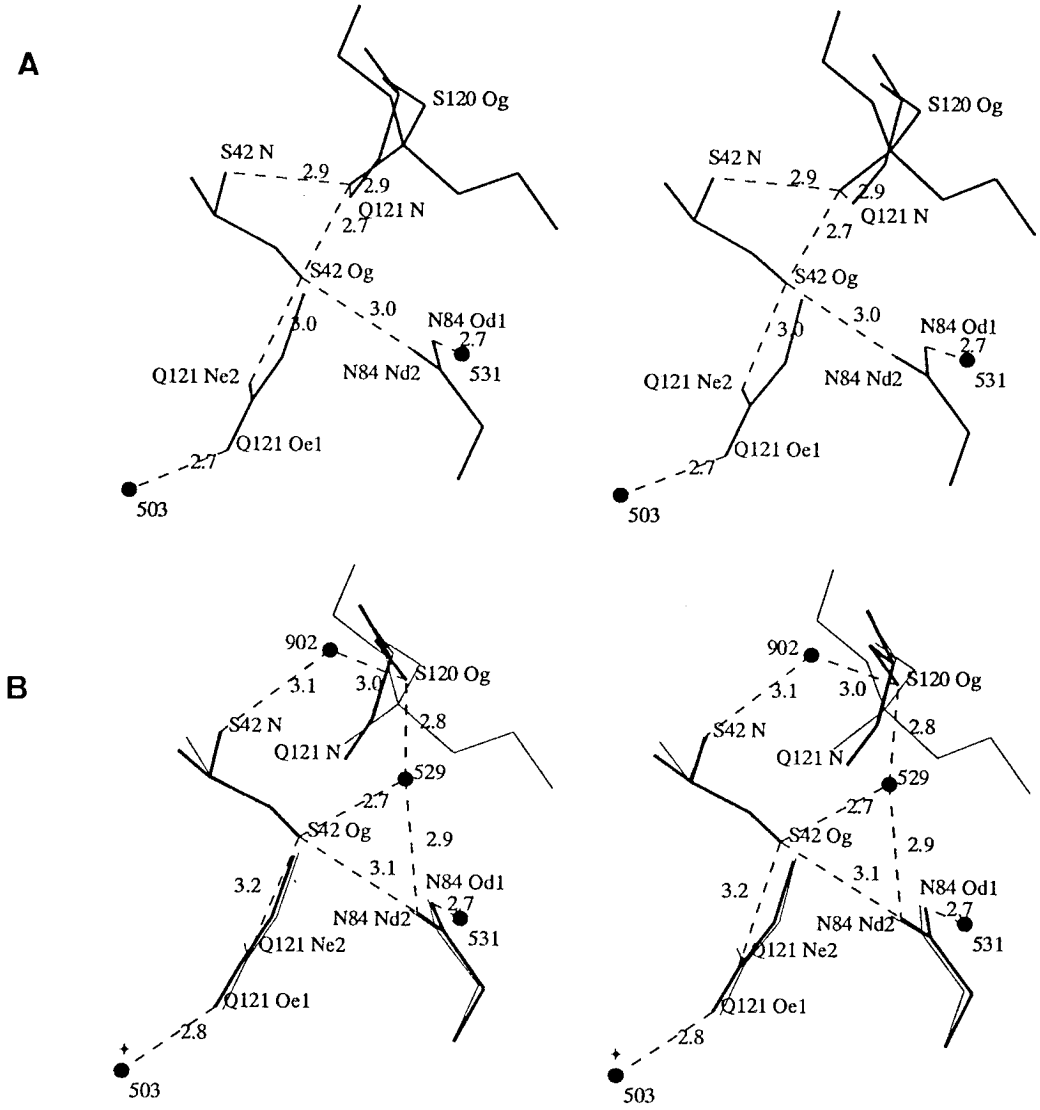

FIGURE 2: (A) Stereoview of the oxyanion hole of E600 inhibited cutinase. Atoms from residues involved in the tetrahedral intermediate stabilization are indicated by hydrogen bonds with the oxyanion. (B) Stereoview of the oxyanion hole of E600 inhibited cutinase (thin) superimposed on that (thick) of native cutinase.

hydrogen bonded to its Oγ atom (2.75 Å) (Figure 2B). This solvent molecule (W529) located at the bottom of the catalytic pocket is topologically equivalent to the oxyanion, since it is located at 0.93 Å from the (P)-O3 oxygen in the complex with E600 (Figure 2B). Although this water molecule is tricoordinated, its *B* factor remains high (33 Å^2), reflecting some disorder or partial occupancy. Residues Leu81 and Val184 form a bridge over the active site groove (Martinez et al., 1992b). Two pockets were identified on either side of this bridge: one of them has Ser120 Oγ and Ser42 Oγ at the bottom, and the other is lined by the Asn84 side chain. In the structure of the E600 inhibited cutinase, the inhibitor is docked under this bridge and fills both pockets.

Mutant S42A. The structure of the S42A mutant active site does not display any drastic changes as compared to that of the native enzyme (Figure 3A). The geometry of catalytic triad Ser120, His188, and Asp175 has not been altered (Tables 3 and 4), and the position of the Ala42 Cβ atom is that of the wild-type serine Cβ. Furthermore, the main chain NH groups of Ser42 and Gln121 are still in a favorable position to form hydrogen bonds with the oxyanion. Due to the absence of the Oγ atom, however, the second hydrogen bond shell established in the wild-type enzyme between Asn84 Nδ2, Gln121 Nϵ2, and Ser42 Oγ is completely lost in the structure of the mutant. This mutant still has the same double position in the case of its N84 Nδ2 atom (position B in Figure 3A) as in the native structure (not shown in the figure). The position of N84 Oδ1 is conserved among all the mutants, due to the hydrogen bond with the water molecule W531. The water molecule (W529) observed in the active site crevice, close to the position of the oxyanion, keeps its position at the bottom of the pocket. The mutation S42A results in the loss of an Oγ atom and leads to the extension of the active site pocket, where a second water molecule (W860) is visible at the top of the pocket (Figure 4A). W529 still maintains its hydrogen bonds with the backbone amide groups of residues 42 (2.97 Å), and 121 (2.98 Å) and with the side chain Oγ of the active Ser (2.60 Å); it establishes a new hydrogen bond with the extra water molecule W860 (3.04 Å). In the alternate position B, the tricoordinated water molecule W860 stabilizes the orientation of Asn84 Nδ2 atom through a hydrogen bond (2.90 Å).

The activity of the S42A mutant on pnp-butyrate is drastically reduced to 0.22% relative to level recorded with

Table 3: List of Deviations, Relative to the Wild-Type Enzyme, of Atoms Belonging to Residues Involved in the Catalytic Triad or in the Oxyanion Hole of Inhibited and Mutants Cutinase

	E600	S42A	N84A	N84L	N84W	N84D
			Active Site			
Ser120 Oγ	0.48	0.06	0.30	0.12	0.14	1.16
His188 Nϵ2	0.48	0.12	0.27	0.14	0.03	0.37
His188 Nδ1	0.29	0.06	0.09	0.13	0.11	0.10
Asp175 Oδ1	0.29	0.06	0.09	0.13	0.11	0.10
			Oxyanion			
Gln121 NH	0.30	0.04	0.13	0.15	0.12	0.13
Ser42 NH	0.25	0.03	0.23	0.13	0.03	0.48
Ser42	Oγ, 0.28	Cβ, 0.15	Oγ, 0.27	Oγ, 0.23	Oγ, 1.37	Oγ, 0.62
Asn84	Nδ2, 0.40	Nδ2, 0.91	Cβ, 0.91	Cδ1, 2.31	Cγ, 1.11	Oδ1, 0.88
Gln121 Nϵ2	0.17	0.43	0.09	0.09	0.08	0.18

Table 4: List of Distances (Å) of Atoms Belonging to Residues Involved in the Catalytic Triad of Native and Mutated Cutinase

	S120 (Oγ)−H188 (Nϵ2)	H188 (Nδ2)−D175 (Oδ1)
wild	2.78	2.91
E600	2.94	2.91
S42A	2.88	2.88
N84A	3.13	2.93
N84L	2.78	2.91
N84W	2.77	2.89
N84D	3.89	2.87

the native enzyme (Table 1). This decrease is due to the collapse of k_{cat}, by a factor of about 450, whereas the K_M remains almost constant. These data provide direct evidence that this residue plays an essential role in stabilizing the transition state oxyanion and that the S42A mutant keeps its affinity for the substrate.

Mutations of Asn84. Asn84 Nδ2 is a rather solvent-exposed atom (with a water accessibility of 5.29 Å^2) with an above average *B* factor (18.46 Å^2). Moreover, the high resolution maps show that Asn84 Nδ2 has two alternate positions (A. Nicolas, unpublished results). In position A (Figure 2B), Asn84 is involved in stabilizing the orientation of the Ser42 side chain through a hydrogen bond with N84 Nδ2 atom (3.1 Å); Nδ2 atom itself is stabilized by means of two other hydrogen bonds, the one with a water molecule close to the active serine (2.9 Å), and the other with Leu81 carbonyl oxygen (2.80 Å). Position B is stabilized by two hydrogen bonds involving water molecules. N84 Oδ1, on the contrary, has an accessibility of 0.29 Å^2 and a *B* factor of 15.36 Å^2, and it does not have a double position. It is stabilized via a single hydrogen bond (2.71 Å) with a tetracoordinated water molecule (W531; *B* factor of 10.15 Å^2). The location of Asn84 close to the enzyme surface and its hydrogen bonding with Ser42 Oγ makes it a good candidate for checking various substitutions leading to electrostatic or steric modifications in the vicinity surrounding the oxyanion hole.

N84A and N84L. Mutations N84A and N84L were designed to disrupt two hydrogen bonds, Asn84 Nδ2 with Ser42 Oγ and Asn84 Oδ1 with the tetracoordinated water molecule W531, without introducing any significant electrostatic or steric modifications. Mutant N84A loses these two hydrogen bonds, and an empty space is created near the active site crevice (Figure 3B). Mutant N84L also loses its two hydrogen bonds, but it is almost isosteric with Asn (Figure 3C). The structures of the N84A and N84L mutant active sites do not display any drastic changes. The catalytic triad involving Ser120, His188, and Asp175 shows no change, and these residues have deviations of only 0.19 Å in the case of N84A and 0.13 Å in that of N84L (Table 3); the catalytic triad hydrogen bonds remain unchanged (Table 4). Furthermore, the oxyanion can still be stabilized by hydrogen bonds with the NH groups of Ser42 and Gln121 and also by the Ser42 side chain. In the second shell of hydrogen bonds, the Gln121 Nϵ2 atom alone establishes a hydrogen bond with Ser42 Oγ. The most significant differences between N84A and N84L result from differences in the bulkiness of the side chain between alanine and leucine. Since the Leu84 side chain is not stabilized by any hydrogen bonds, it drifts into the active site pocket. The mutation of N84A results, as with S42A, in the loss of an oxygen atom, which is replaced by a water molecule, W860. W529 loses its hydrogen bond with both backbone amides but still keeps its hydrogen bonds with the Oγ atom of the catalytic serine (3.04 Å) and with the Oγ of Ser42 (2.49 Å); it also establishes a hydrogen bond with the water molecule W860 (3.12 Å). Despite the fact that water molecule W860 is tricoordinated, as in the S42A mutant, its hydrogen bonding network is different, which indicates the existence of contacts with Ser120 Oγ (2.70 Å), His188 Nϵ2 (2.78 Å), and water 529. The catalytic pocket of the N84L mutant contains the water molecule W529, but in a position which has shifted to the opposite side of the second pocket, as compared with the native structure. Water molecule W529 still maintains its hydrogen bonds with backbone amide groups of residues 42 (2.97 Å), with the side chain Oγ of the active Ser120 (2.60 Å) and with Ser42 Oγ (2.60 Å).

In mutant N84L, the side chain of Leu 84 is no longer stabilized by a hydrogen bond and occupies the second solvent cavity. Compared to the N84L mutant, the Ala84 side chain has lost this hydrogen bond but does not fill the cavity. The 12% decrease in the activity of N84L as compared to N84A is probably due to this steric hindrance. In the native structure, the tetracoordinated water molecule W531 stabilizes Asn84 Oδ1 in a single position despite the double position of Asn84 Nδ2. It was particularly interesting to note that W531 is located at the bottom of the deepest and most narrow crevice of cutinase (diameter of 3.01 Å and depth of 5.71 Å). This water molecule is present in all the mutant structures.

The residual activities of mutants N84A and N84L are quite appreciable: N84A still retains 26.5% of the activity of the wild-type enzyme, whereas N84L retains only 3.0% (Table 1). This catalytic behavior of the N84L mutant is quite surprising, since it is also due to a decrease in k_{cat} and not to an increase in the K_M, which remains constant. This rules out the possibility that the mutation may have steric

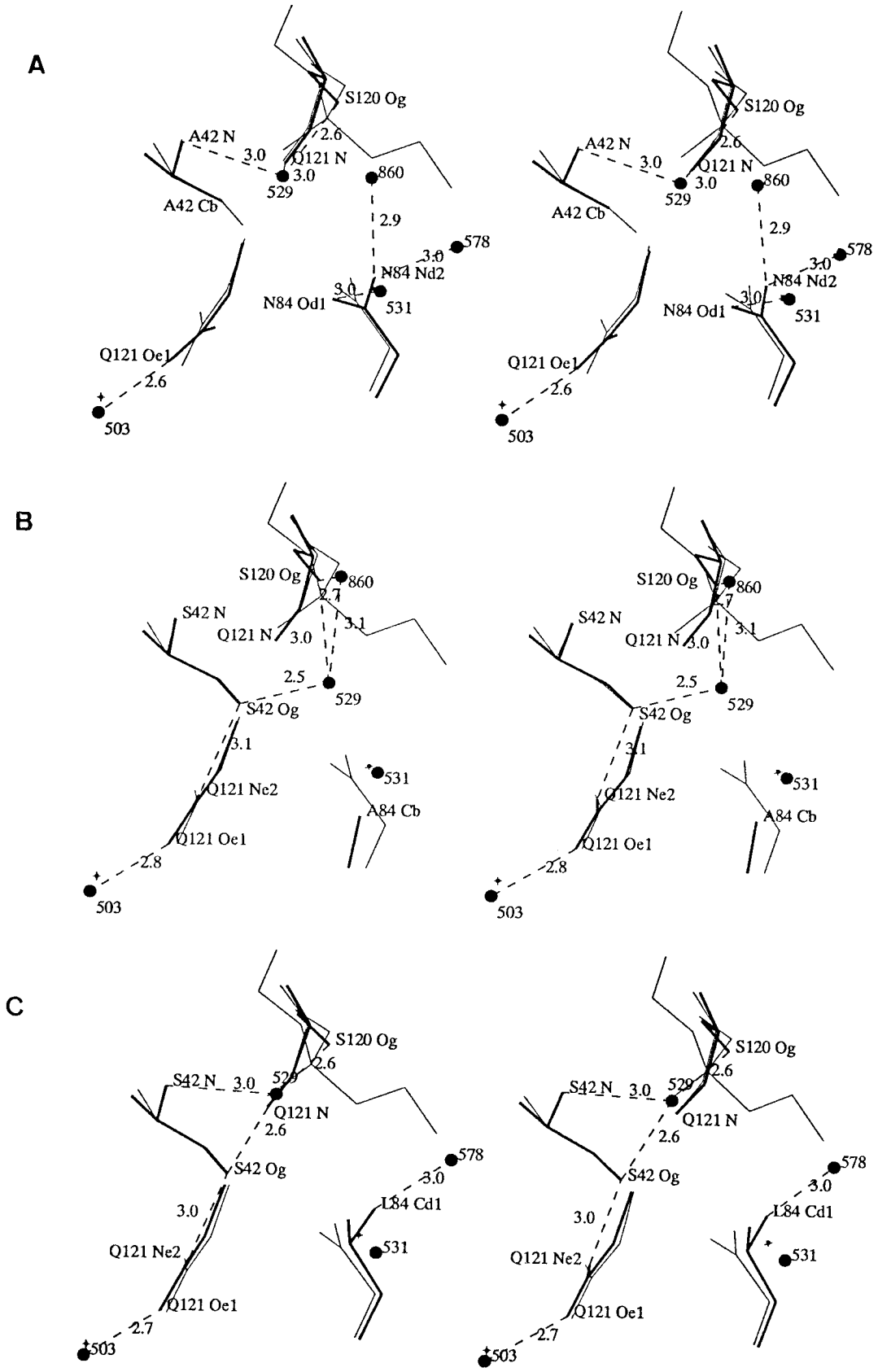

effects on the substrate docking. The overall kinetic effect may therefore be due to the sum of numerous small changes on the structure and dynamics of the active site as a whole.

N84D. Mutation Asn84 in Asp84 results in the introduction of a negative charge into the oxyanion hole pocket. Since Asn and Asp are isosteric, neither steric clashes nor cavity formation are liable to complicate the interpretation of the kinetic results. Despite this isostericity, mutant N84D is the only one that crystallizes in a different space group: this is probably due to the electrostatic effects of the mutation on the crystal packing. This effect has often been noted with cutinase mutants having charge differences (S. Longhi and A. Nicolas, unpublished results). The negative charge introduced by Asp into the active site pocket induces different

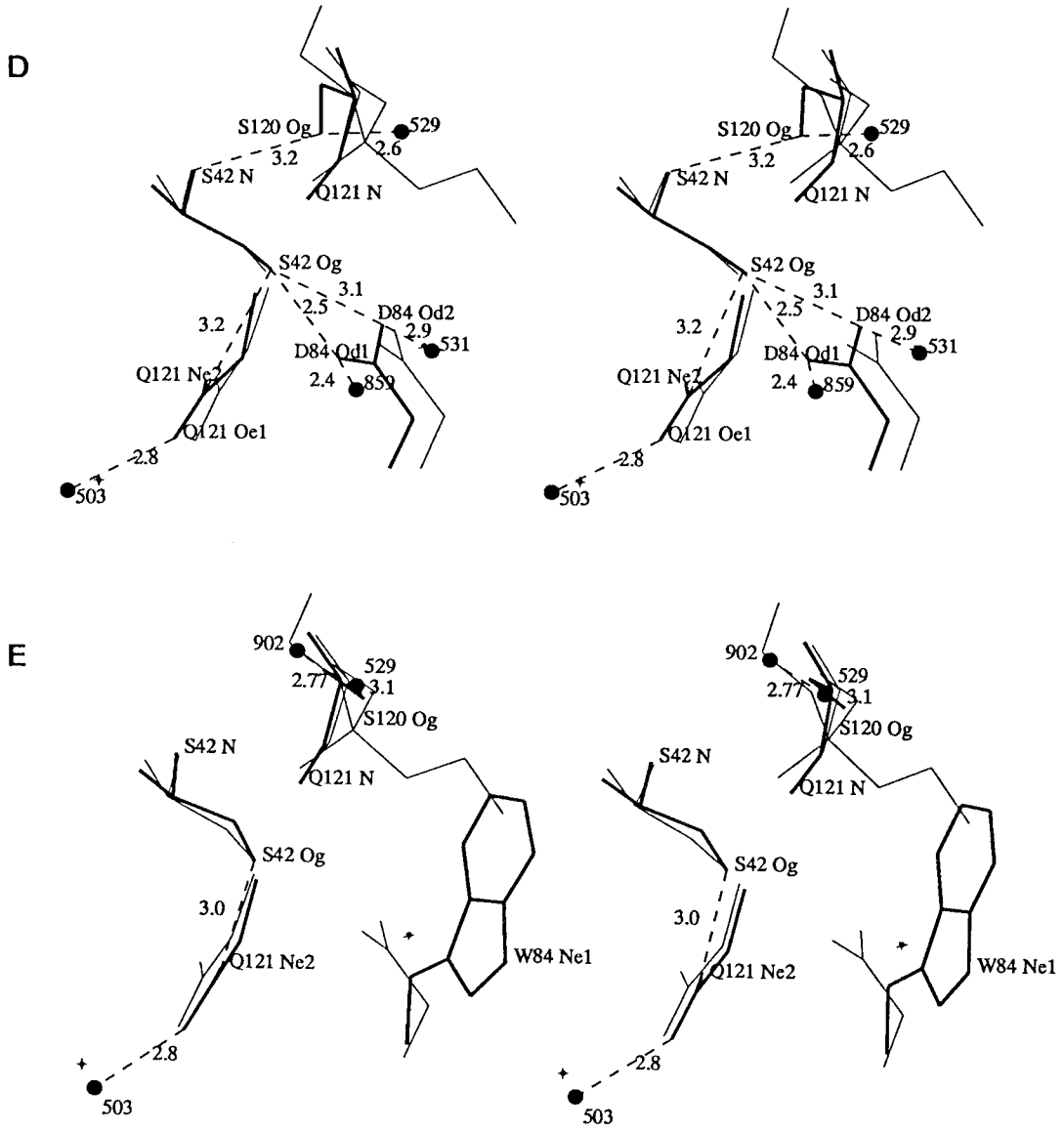

FIGURE 3: Stereoview of the oxyanion hole of E600 inhibited cutinase (thin) superimposed on that (thick) of S42A (A) and those of mutants N84A (B), N84L (C), N84D (D), and N84W (E).

stereochemical changes in its vicinity, together with a movement of the Arg208 side chain from a symmetry-related molecule toward the active site (Figure 4). The symmetry-related Arg208 side chain is stabilized by two hydrogen bonds with Tyr119 OH and with the active site water molecule W529, which itself is hydrogen-bonded to Ser120 Oγ. The symmetry-related C-terminal helix (Glu201 to Ser213) and a β-turn (Ser57 to Ala62) are consequently located close to three loops (Thr43 to Thr45, Leu81 to Gly89, Ile183 to Leu189) surrounding the active site. The overall structural modifications observed result mainly from the new crystallographic packing.

Concerning the active site residues, Ser42 Oγ establishes hydrogen bonds with Asp84 Oδ2 and Asp84 Oδ1. In the native cutinase, Ser42 Oγ plays the role of the acceptor for the hydrogen bond with Asn84 Nδ2 and donor for the hydrogen bond with the oxyanion. In the crystallization and activity measurement buffers (pH 7 and 9, respectively), Asp84 side chain is deprotonated. Ser42 Oγ therefore becomes the donor in a very tight hydrogen bond with Asp84 Oδ2 (2.5 Å), indicating that Ser42 Oγ hydrogen is not available for oxyanion stabilization (Figure 3D). The hydrogen bond established between Ser42 Oγ side chain and Gln121 Nϵ2 is weaker (3.2 Å) than that between Ser42 Oγ side chain and Asn84 Oδ2. The shift of Ser42 Oγ leads to the shift of the loop Thr 43 to Thr45. The catalytic Ser120 Oγ is shifted 1.44 Å as compared with the wild-type enzyme and forms a hydrogen bond with Ser42 NH and symmetrical Arg208 Nϵ2 via the water molecule W529. The shift of Ser120 Oγ results from the introduction of Arg208 into the active site. Although the geometry of the oxyanion hole main chain NH groups remains intact, the catalytic triad geometry is severely disturbed, since Ser120 Oγ is located 3.89 Å from His188 Nη2 (Table 4). The narrow bridge involving Leu81 with Val184 no longer exists, so that there exists a continuum between the two solvent-accessible pockets of the active site crevice, where three water molecules become visible. Leu81 displays the most striking shift as compared with the position in the native enzyme, in which Leu81 O is hydrogen-bound to Asn84 Nδ2. In the mutant N84D, Asp84 Oδ2 generates a repulsive effect toward Leu81 carbonyl oxygen, resulting in a 180° rotation of its main chain. Consequently, Leu81 NH also rotates through 180° and establishes a hydrogen bond with a symmetry

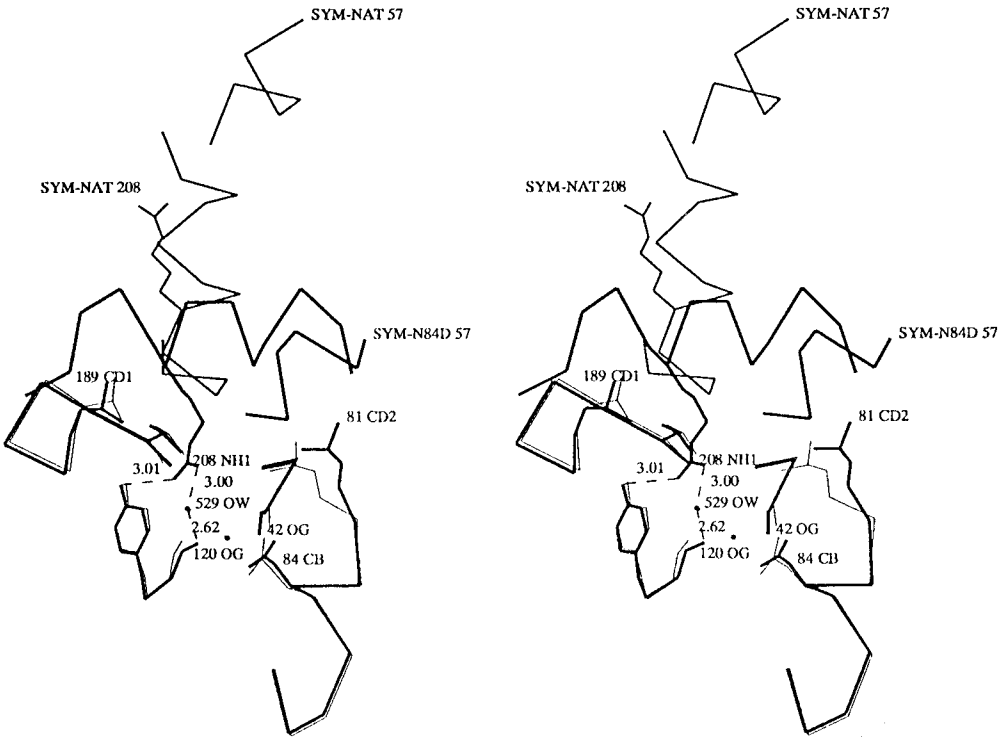

FIGURE 4: Stereoview of the intermolecular interactions between the structure of the N84D mutant and a symmetrical related molecule in the region of the catalytic serine superimposed with the native ones. By thickness decrease: N84D mutant, N84D symmetrical related, native symmetrical related, and native molecule. When not indicated, the labeled atoms are those of the N84D molecules.

related Glu201 Oϵ2 atom. Water molecule W529 is shifted from its original position, near the inhibitor (P)-O3 oxygen position, at the bottom of the catalytic crevice, to a new position close to the water molecule W860 observed in the structure of mutants N84A and S42A. It displays the same hydrogen bond network as water molecule W860, being in contact with Ser120 Oγ (2.62 Å), His188 Nϵ2 (2.79 Å), and W866.

As may be expected in the case of such drastic structural changes, the catalytic activity is greatly reduced using pnp-butyrate, to only 0.13% relative to that observed with the wild-type enzyme (Table 1). The large decrease in k_{cat} supports the idea that an electrostatic destabilization of the transition state may be introduced by the charge modification into the oxyanion hole pocket.

N84W. In the closed conformations of RmL and Human pancreatic lipase (HPL), a Trp residue belonging to the lid blocks the accessibility of the active serine. This Trp moves when the substrate binding occurs, following the movement of the lid. Replacing Asn84 in cutinase by a Trp restores the steric features observed in the closed form of these two lipases. This mutation was investigated in an attempt to induce a structural rearrangement of the enzyme, mimicking the structural rearrangements which occur in response to the interfacial activation of lipases. No such rearrangement was obtained, however, either structurally or kinetically. As can be seen from Figure 3E, Trp84 entirely fills the second solvent-accessible pocket. Hydrophobic interactions occur with Leu81 and Leu182, which stabilize the Trp ring in its orientation, as the result of which the active serine is completely hidden and the water molecule, which is normally bond to Oγ, is moved from the bottom to the top of the pocket; a second water molecule, W902, stabilizes Ser120 Oγ. In the second shell of interactions, the hydrogen bond between Ser42 Oγ and Gln121 Nϵ2 is the only stabilizating interaction which is conserved. The conformation of the catalytic triad and that of the oxyanion hole components are conserved, however (Tables 3 and 4). Water molecule W529 displays the same behavior as in the N84D mutant and is in contact with Ser120 Oγ (3.07 Å), His188 Nϵ2 (3.18 Å), and W664.

This mutation leads to a residual catalytic activity of 0.11%, the lowest obtained among all the variants studied so far (Table 1). Kinetic experiments performed on C3 and C4 triglycerides (A. Nicolas, unpublished results) showed the occurrence of a dramatic decrease in activity, working from the C3 to the C4 alkyl chain length substrates. This suggests that no structural rearrangement is possible in the vicinity of the cutinase active site crevice, but that the N84W cutinase can accommodate very small C3 substrates and still be active on them. This result confirms without any doubt that acute steric hindrance is exerted toward the substrate by the Trp mutation.

DISCUSSION

Among the nucleophile-His-Asp (Glu) proteases, trypsin (Stroud et al., 1974), chymotrypsin (Blow, 1976), and *Streptomyces griseus* proteinase A (Blanchard & James, 1994), a chymotrypsin-like enzyme, the oxyanion is stabilized by two main chain nitrogen groups, while in subtilisin (Steinmetz et al., 1994) and papain (Schöder et al., 1993) one of the nitrogen groups comes from the main chain and the other from a side chain (Table 5). Proteases have their triad in the opposite handedness to that of lipases. Consequently, this change reverses the direction of the polypeptide backbone around the His and Ser residues. The amide NH oxyanion component of the nucleophile residue in proteases becomes equivalent to the amide NH of the following residue in lipases. It can be noted that, in serine carboxypeptidases alone among all the proteases, the first NH has the same

Table 5: List of Oxyanion Stabilization Components of Some Enzymes Mentioned in the Text.

nucleophile-His-Asp (Glu) hydrolase with its (nucleophilic residue)		main chain group			side chain group	
		1st NH	2nd NH	3rd NH	NH	OH
serine protease						
trypsin	(S195)	S195	G193			
chymotrypsin	(S195)	S195	G193			
proteinase A	(S195)	S195	G193			
subtilisin	(S221)	S221			N155 Nδ2	
carboxypeptidase II	(S146)	S147	G53			
cysteine protease						
papain	(C25)	C25			Q19 Nϵ2	
esterase						
Streptomyces scabies esterase	(S14)	S14	G66		N106 Nδ2	
acetylcholinesterase	(S200)	A201	G118	G119		
lipase						
Candida rugosa lipase	(S209)	A210	G124	G123		
human pancreatic lipase	(S152)	L153	F77			
horse pancreatic lipase	(S152)	L153	F77			
Pseudomonas glumae lipase	(S87)	Q88	L17			
Mucor miehei lipase	(S144)	L145	S82			S82 Oγ
Penicillium camembertii lipase	(S145)	L146	S81			S81 Oγ
Humicola lanuginosa lipase	(S146)	L147	S83			S83 Oγ
Rhizopus delemar lipase	(S145)	L146	T83			T83 Oγ1
Candida antartica B lipase	(S107)	Q106	T40			T40 Oγ1
cutinase	(S120)	Q121	S42			S42 Oγ

feature as that observed in lipases (Liao & Remington, 1990). In all the known esterase structures, acetylcholinesterase (Sussman et al., 1991), and *Streptomyces scabies* esterase (Wei et al., 1995), and in *Candida rugosa* lipase (CRL) (Grochulski et al., 1994), which is the lipase structurally homologous with acetylcholine, three amide groups stabilize the oxyanion hole, namely, three main chain groups and two main chain groups with a side chain group, respectively (Table 5). Up to now, among those lipases the three-dimensional structure (except CRL) of which is known in their inhibited form, two schemes of oxyanion stabilization have been found to exist (Table 5). Both cases show a common hydrogen bonding network arising from two main chain nitrogen groups. In HPL (Egloff et al., 1995), horse pancreatic lipase (Bourne et al., 1994), and *Pseudomonas glumae* lipase (Noble et al., 1994), the oxyanion stabilization components belong to this first scheme. In the second scheme, a third hydrogen bond occurs through a serine or threonine side chain hydroxyl group. The serine Oγ component is present in *Rhizomucor miehei* lipase (RmL) (Brzozowski et al., 1991), *Penicillium camembertii* lipase (PcL) (Derewenda et al., 1994; Yamaguchi et al., 1992), *Humicola lanuginosa* lipase (HlL) (Derewenda et al., 1994), and cutinase (Martinez et al., 1994); the threonine hydroxyl group is present in *Rhizopus delemar* lipase (RdL) (Derewenda et al., 1994; Joerger & Haas, 1994) and *Candida antartica* B (CaBL) (Uppenberg et al., 1994). The reason why serine and cysteine proteases require two amide groups, whereas esterases and CRL require three amide groups, some lipases require two amide groups, and other lipases require two amide groups and a hydroxyl group in the oxyanion hole is puzzling. Four hydrolases have been investigated to date by performing site-directed mutagenesis to study kinetically the importance of a side chain residue involved in the oxyanion hole stabilization. In the serine protease subtilisin BPN′, the mutation of Asn155 into Leu (Bryan et al., 1986) resulted in a decrease in the k_{cat} toward peptidyl substrate. In the cysteine protease papain, the mutations of Gln19 into Ala or Ser (Ménard et al., 1991) resulted in the decrease of k_{cat} toward CBZ-Phe-Arg-MCA, a peptidyl substrate. In cutinase, mutation Ser42 into Ala also has a marked effect on the k_{cat} but causes only minor changes on the Michaelis constant. In RdL, mutations of Thr83 into Ala or Ser (Joerger & Haas, 1994) and, in PcL, the mutation of Ser84 into Gly (Yamaguchi et al., 1992) lead to a decrease in the specific activity toward several triglyceridyl substrates.

The present study is the first attempt made so far to analyze the effects of the mutations on the three-dimensional structures of the oxyanion hole compounds from the kinetic point of view. The finding that the cutinase mutation S42A drastically reduces the enzyme activity demonstrates that Ser42 Oγ plays an essential role in stabilizing the oxyanion of the tetrahedral intermediate. The loss of transition state binding free energy, $\Delta\Delta G^{\ddagger}$, due to a site-directed mutation, can be calculated from the kinetic constants, k_{cat} and K_M, using the equation $\Delta\Delta G^{\ddagger} = -RT \ln[(k_{cat}/K_M)^{mutant}/(k_{cat}/K_M)^{wild\text{-}type}]$ (Fersht et al., 1985). Using this equation, the hydrogen bond of Ser42 Oγ with the oxyanion contributes about 3.3 kcal mol^{-1} to the stabilization of the transition state. The Asn155 side chain in subtilisin, Gln19 in papain, and Gln195 in tyrosyl-tRNA synthetase are also involved in the stabilization of an oxyanion in the transition state. The loss of transition state binding free energy is in the range 2.2−4.8 kcal mol^{-1} in the case of the subtilisin variants N155X (Bryan et al., 1986; Wells et al., 1986; Rao et al., 1987; Carter & Wells, 1990), 2.4−3.8 kcal.mol^{-1} in that of the papain variants Q19X (Ménard et al., 1991), and 3−6 kcal mol^{-1} in that of the tyrosyl-tRNA synthetase variants Q195X (Fersht et al., 1985). It has been suggested by Fersht (Fersht et al., 1985) that if a hydrogen bond deletion occurs between a side chain and a charged group on the substrate, the binding free energy changes will be within the 3−6 kcal mol^{-1} range. With the subtilisin, papain, and tyrosyl-tRNA synthetase variants as well as with the cutinase S42A variant, the loss of the hydrogen bond due to the mutation involves a charged group of the substrate (C−O$^-$), which is present in the transition state, and the values observed are within the range proposed by Fersht.

Table 6 gives, for cutinase, subtilisin, and papain, the kinetic parameters observed upon mutating into an alanine

Table 6: Kinetic Parameters of Wild and Mutant Cutinase, Subtilisin, and Papain and Energetic Contribution of the Side Chain to the Stabilization of the Oxyanion in the Transition State

	substrate	k_{cat} (s^{-1})	k_{cat}/K_M (s^{-1} mM^{-1})	% residual activity	$\Delta\Delta G^{\ddagger}$(kcal mol^{-1})
cutinase					
WT	pnp-butyrate	1800	2647	100	
S42A		4	12	0.22	3.3
subtilisin					
WT	Ala-Ala-Phe	50	357	100	
N155A		0.11	0.36	0.22	3.7
papain					
WT	CBZ-Phe-Arg-MCA	41.6	464	100	
Q19A		2.4	7.7	5.8	2.4

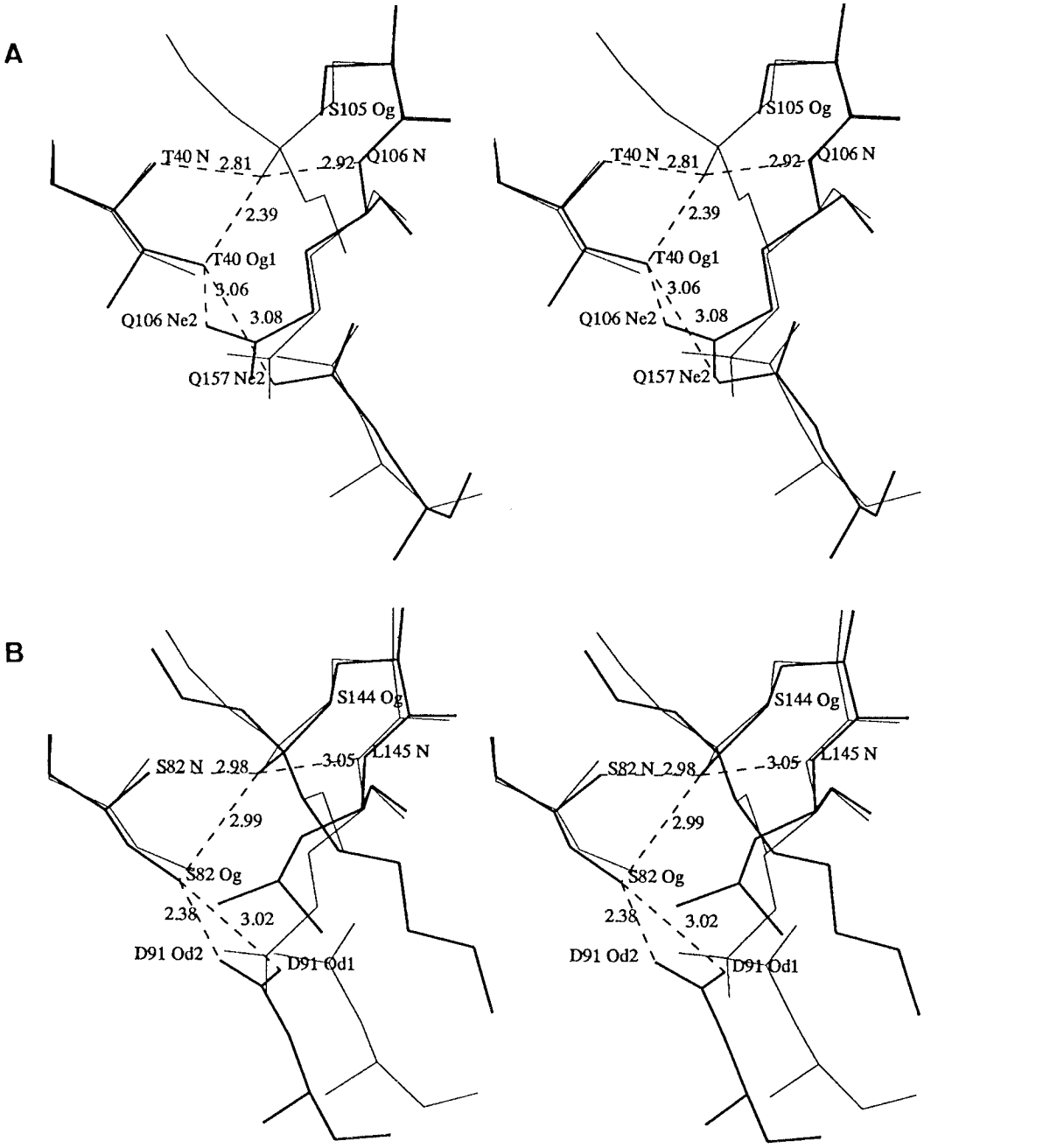

FIGURE 5: Stereoview of the oxyanion hole of E600 inhibited cutinase (thin) superimposed on that (thick) of the CaBL (A) and on that of the C6−RmL complex (B). Only the significant hydrogen bonds have been included.

residues stabilizing the substrate oxyanion in the transition state. The residual activity and the loss of transition state binding free energy were found to be quite similar between subtilisin mutant N155A and cutinase mutant S42A. With the papain mutant Q19A, the value of the residual activity was higher and the loss of transition state binding free energy was lower than those observed with mutants S42A and N155A. These kinetic differences cannot have been attributable to structural differences between the mutants S42A, Q19A, and N155A analyzed through (i) the nature of the

lost side chain stabilizing the oxyanion, (ii) the size of the side chain fragment removed, and (iii) the number of hydrogen bonds that continue to stabilize the oxyanion. In both subtilisin and papain, the side chain group involved in the stabilization of the oxyanion is an amide group, whereas in cutinase it is a hydroxyl group. In mutants N155A and Q19A, the size of the fragments removed, $CONH_2$ and CH_2-$CONH_2$, respectively, are quite similar, whereas, in the S42A mutant, this fragment, an OH, is clearly smaller than those of mutants N155A and Q19A. In N155A and Q19A mutants, only one hydrogen bond remains to stabilize the oxyanion, whereas, in the S42A mutant, two hydrogen bonds are left. It therefore seems likely that mutants N155A and Q19A are most similar from the structural point of view, whereas, from the point of view of kinetics, the similarity was observed between mutants N155A and S42A. Ménard et al. (1991) have suggested that the difference observed between the kinetic parameters of mutants N155A and Q19A may reflect the fact that the extent of transition state stabilization achieved through the oxyanion hole of papain, although highly significant, is somewhat smaller than that achieved through a comparable interaction in subtilisin.

Cutinase mutations N84W, N84L, and N84A disrupt the hydrogen bond stabilization of Asn84 Nδ2 with Ser42 Oγ and modify the steric environment in the active site pocket. The activity on pnp-butyrate is reduced to 0.11% in the Trp mutant as compared with the wild-type enzyme and remains at 3% and 26.5% with Leu and Ala mutants, respectively. As the result of these three mutations with nonpolar residues, the catalytic triad and the oxyanion hole geometry remain unchanged. Gln121 superimposes with the wild-type enzyme and maintains Ser42 Oγ in the appropriate orientation to be properly oriented in the oxyanion stabilization. The fact that mutation N84W leads to the lowest residual activity as compared with the wild type confirms that the steric increase introduced by the Trp ring blocks the access to the active site as far as the medium sized (C4) ester substrates, but not the smallest ones, are concerned (C3). The introduction of a net negative charge into the oxyanion hole pocket resulting from the N84D mutation modifies the hydrogen bonding network in the catalytic triad and the oxyanion hole. The hydrogen bond stabilization of the oxyanion with Ser42 Oγ and Ser120 Oγ with His188 Nϵ2 is disrupted. The activity on pnp-butyrate is reduced to 0.13% as compared with that of the wild-type enzyme, which is similar to what occurs with the N84W mutant. Asn84 appears to play a significant role in the electrostatic stabilization of the active site pocket but seems not to be absolutely essential because mutants Asn84Leu and Asn84Ala continue to have some esterase activity. Asn84 does show a change in the k_{cat} but only minor changes in the Michaelis constant.

With a view to determining whether or not the geometry of the cutinase oxyanion hole can be taken to apply in the case of other lipases, we performed structural comparisons among several lipases. In some lipases, the second oxyanion hole nitrogen component becomes properly positioned only after a conformational change. Upon superimposing the catalytic triad and the two oxyanion hole main chain NH groups of the open form of lipases mentioned in the introduction (data not shown), an excellent structural fit was observed between them. Only a few of them have a hydroxyl group on the second residue of the oxyanion hole, however, namely, RmL and the homologous RdL, PcL and HlL, CaBL and cutinase. The three dimensional structure of cutinase−E600 complex (Martinez et al., 1994) was superimposed on that of the RmL-*n*-hexylphosphonate ethyl ester complex (RmL-C6) (Brzozowski et al., 1991) and on that of CaBL (Uppenberg, 1994) using the rigid body option of the TURBO software program (Roussel & Cambillau, 1991). In RmL, the second oxyanion NH component is Ser82, located within the lid hinge. In CaBL, Thr40 NH is already in a suitable conformation for catalytic activity to occur, since this lipase shares with cutinase the property of having an open active site. Superimposing the oxyanion hole components (Ser42 N, Gln121 N, and Ser42 Oγ) of cutinase onto structurally corresponding atom positions in RmL and CaBL gives root mean square deviations of 0.23 and 0.09 Å, respectively. Residue Thr40 of CaBL has not yet been studied yet, but the oxyanion hole geometry is the most similar so far to that of cutinase and has the same three interaction shells (Figure 5A). The role of RmL Ser82 Oγ in stabilizing the oxyanion hole can be inferred from the results obtained on mutants RdL Thr83 (Joerger & Hass, 1994) and mutants PcL Ser84 (Yamaguchi et al., 1992) since these residues are homologous to RmL Ser82 (Derewenda, 1994). The results of our kinetic experiments and structural analysis of these cutinase mutants provide new evidence supporting the idea that Ser42 Oγ is an extra component of the cutinase oxyanion hole, acting in combination with the two main chain nitrogen atoms 42 and 121. The reason why cutinase and some lipases need three hydrogen bonds to stabilize the oxyanion, while subtilisin and other lipases need only two, still remains to be elucidated, however.

REFERENCES

Abergel, C., Martinez, C., Fontecilla-Camps, J., Cambillau, C., De Geus, P., & Lauwereys, M. (1990) *J. Mol. Biol. 215*, 215−216.

Blanchard, H., & James, M. N. G. (1994) *J. Mol. Biol. 241*, 574−587.

Blow, D. M. (1976) *Acc. Chem. Res. 9*, 145−152.

Bourne, Y., Martinez, C., Kerfelec, B., Lombardo, D., Chapus, C., & Cambillau, C. (1994) *J. Mol. Biol. 238*, 709−732.

Brady, L., Brzozowski, A., Derewenda, Z. S., Dodson, R., Dodson, G., Tolley, S., Turkenburg, J. P., Christiansen, L., Huge-Jensen, B., Norskov, L., Thim, L., & Menge, U. (1990) *Nature 343*, 767−770.

Brünger, A. T. (1992) *X-PLOR Manual, Version 3.1*, Yale University Press: New Haven, CT.

Brünger, A. T., Karplus, M., & Petsko, G. (1989) *Acta Crystallogr. A45*, 50−61.

Bryan, P., Pantoliano, M. W., Quill, S. G., Hsiao, H., & Poulos, T. (1986) *Proc. Natl. Acad. Sci. U.S.A. 83*, 3743−3745.

Brzozowski, A. M., Derewenda, U., Derewenda, Z. S., Dodson, G., Lawson, D., & Turkenburg, J. P. (1991) *Nature 351*, 491−494.

Carter, P., & Wells, J. A. (1990) *Proteins: Struct., Funct., Genet. 7*, 335−342.

Derewenda, U., Swenson, L., Green, R., Wei, Y., Yamaguchi, S., Joerger, R., Haas, M. J., & Derewenda, Z. S. (1994) *Protein Eng. 7*, 551−557.

Duggleby, R. G. (1981) *Anal. Biochem. 110*, 9−18.

Dulau, L., Cheyrou, A., & Aigle, M. (1989) *Nucleic Acids Res. 17*, 2873.

Egloff, M.-P., Marguet, F., Buono, G., Verger, R., Cambillau, C., & van Tilbeurgh, H. (1995) *Biochemistry 34*, 2751−2762.

Engh, R. A., & Hubert, R. (1991) *Acta Crystallogr. A47*, 392−400.

Fersht, A. R., Shi, J. P., Knill-Jones, J., Lowe, D. M., Wilkinson, A. J., Blow, D. M., Brick, P., Waye, M. M. Y., & Winter, G. (1985) *Nature 314*, 235−238.

Grochulski, P., Li, Y., Schrag, J. D., Bouthillier, F., Smith, P., Harrison, D., Rubin, B., & Cygler, M. (1993) *J. Biol. Chem. 268*, 12843−12847.
Grochulski, P., Bouthillier, F., Kazlauskas, R. J., Serreqi, A. N., Schrag, J. D., Ziomek, E., & Cygler, M. (1994) *Biochemistry 33*, 3494−3500.
Ho, S. N., Hunt, H. D., Horton, R. M., Pullen, J. K., & Pease, L. R. (1989) *Gene 77*, 51−59.
Jaeger, K. E., Ransac, S., Dijkstra, B. W., Colson, C., van Heuvel, M., & Misset, O. (1994) *FEMS Microbiol. Rev. 15*, 29−63.
Joerger, R. D., & Haas, M. J. (1994) *Lipids 29*, 377−384.
Kadowaki, H., Kadowaki, T., Wondisford, F. E., & Taylor, S. I. (1989) *Gene 76*, 161−166.
Kabsch, W. (1988) *J. Appl. Crystallogr. 21*, 916−924.
Kolattukudy, P. E. (1984) in *Lipases* (Borgström, B., & Brockman, H., Eds.) pp 471−504, Elsevier, Amsterdam.
Kraut, J. (1977) *Annu. Rev. Biochem. 46*, 331−358.
Lauwereys, M., de Geus, P., de Meutter, J., Stanssens, P., & Matthyssens, G. (1991) in *Lipases—Structure, Mechanism and Genetic Engineering* (Alberghina, L., et al., Eds.) Vol. 16, pp 243−251 VCH, Weinheim.
Liao, D.-L., & Remington, S. J. (1990) *J. Biol. Chem. 265*, 6528−6531.
Lopes, T. S., Klootwijk, J., Veenstra, A. E., van der Aar, P. C., van Heerikhuizen, H., Raue, H. A., & Planta, R. J. (1989) *Gene 79*, 199−206.
Martinez, C. (1992) Thèse de doctorat, Université de Paris XI, Orsay, France.
Martinez, C., de Geus, P., Lauwereys, M., Matthyssens, G., & Cambillau, C. (1992) *Nature 356*, 615−618.
Martinez, C., Nicolas, A., van Tilbeurgh, H., Egloff, M.-P., Cudrey, C., Verger, R., & Cambillau, C. (1994) *Biochemistry 33*, 83−89.
Matthews, B. W. (1968) *J. Mol. Biol. 33*, 491−497.
Ménard, R., Carrière, J., Laflamme, P., Plouffe, C., Khouri, H. E., Vernet, T., Tessier, D. C., Thomas, D. Y., & Storer, A. C. (1991) *Biochemistry 30*, 8924−8928.
Navaza, J. (1994) *Acta Crystallogr. A50*, 157−163.
Noble, M. E. M., Cleasby, A., Johnson, L. N., Egmond, M. R., & Frenken, L. G. J. (1994) *Protein Eng. 7*, 559−562.
Ollis, D. L., Cheah, E., Cygler, M., Dijkstra, B., Frolow, F., Franken, S. M., Harel, M., Remington, S. J., Silman, I., Schrag, J., Sussman, J. L., Verschueren, K. H. G., & Goldman, A. (1992) *Protein Eng. 5*, 197−211.
Orr-Weaver, T. L., & Szostak, J. M. (1983) *Mol. Cell Biol. 3*, 747−749.
Pauling, H. (1946) *Chem. Eng. News 24*, 1375−1377.
Rao, S. N., Singh, U. C., Bash, P. A., & Kollman, P. A. (1987) *Nature 328*, 551−554.
Roussel, A., & Cambillau, C. (1991) in *Silicon Graphics Directory* (Silicon Graphics, Ed.) p 97, Mountain View, CA.
Sanger, F., Nicklen, S., & Coulson, A. R. (1980) *Proc. Natl. Acad. Sci. U.S.A. 74*, 5463−5468.
Schrag, J. D., Li, Y., Wu, S., & Cygler, M. (1991) *Nature 351*, 761−764.
Schröder, E., Phillips, C., Garman, E., Harlos, K., & Crawford, C. (1993) *FEBS Lett. 315*, 38−42.
Smith, L. M., Fung, S., Hunkapiller, M. W., Hunkapiller, T. J., & Hood, L. E. (1985) *Nucleic Acids Res. 13*, 2399−2412.
Smith, L. M., Sanders, J. Z., Kaiser, R. J., Hughes, P., Dodd, C., Connell, C. R., Heiner, C., Kent, S. B. H., & Hood, L. E. (1986) *Nature 321*, 674−679.
Steinmetz, A. C. U., Demuth, H.-U., & Ringe, D. (1994) *Biochemistry 33*, 10535−10544.
Stroud, R. M., Kay, L. M., & Dickerson, R. E. (1974) *J. Mol. Biol. 83*, 185−208.
Sussman, J. L., Harel, M., Frolow, F., Oefner, C., Goldman, A., Toker, L., & Silman, I. (1991) *Science 253*, 872−879.
Uppenberg, J., Hansen, M. T., Patkar, S., & Jones, T. A. (1994) *Structure 2*, 293−308.
van Tilbeurgh, H., Sarda, L., Verger, R., & Cambillau, C. (1992) *Nature 359*, 159−162.
van Tilbeurgh, H., Egloff, M.-P., Martinez, C., Rugani, N., Verger, R., & Cambillau, C. (1993) *Nature 362*, 814−820.
Warshel, A., Naray-Szabo, G., Sussman, F., & Hwang, J.-K. (1989) *Biochemistry 28*, 3629−3637.
Wei, Y., Schottel, J. L., Derewenda, U., Swenson, L., Patkar, S., & Derewenda, Z. S. (1995) *Struct. Biol. 2*, 218−223.
Wells, J. A., Cunningham, B. C., Graycar, T. P., & Estell, D. A. (1986) *Phil. Trans. R. Soc. London A317*, 415−423.
Whiting, A. K., & Peticolas, W. L. (1994) *Biochemistry 33*, 552−561.
Winkler, F. K., D'Arcy, A., & Hunziker, W. (1990) *Nature 343*, 771−774.
Yamaguchi, S., Mase, T., & Takeuchi, K. (1992) *Biosci. Biotech. Biochem. 56*, 315−319.

BI9515578